photochem

Photochemistry of β-γ-Unsaturated Spirolactones

Werner Fudickar, Melanie Metz, Tobias Krüger-Braunert, Alexandra Kelling, Eric Sperlich [ID], Pablo Wessig and Torsten Linker *[ID]

Department of Chemistry, University of Potsdam, Karl-Liebknecht-Str. 24-25, 14476 Golm, Germany; werner.fudickar@uni-potsdam.de (W.F.); eric.sperlich@uni-potsdam.de (E.S.); wessig@uni-potsdam.de (P.W.)
* Correspondence: linker@uni-potsdam.de

Abstract: β-γ-unsaturated spirolactones are easily available by Birch reduction. We describe their photochemistry in the presence of or without carbonyl compounds. The spirolactones show a distinct absorption band at 230 nm, which is not present in other cyclohexadienes. We explain this behavior by an interaction of the double bonds with the carbonyl group through space, further proven by TDDFT calculations. This allows their direct excitation with UV-C light. Interestingly, we obtain only products of an oxa-di-π-methane rearrangement, hitherto unknown for lactones. This speaks for a reaction pathway starting from singlet states, confirmed by calculated relative energies of biradical intermediates. Although polymerization is the main side reaction, we were able to isolate tricyclic lactones in moderate yields in a pure form. In the presence of benzaldehyde or benzophenone, excitation with UV-B light was possible, leading to H-atom abstraction in the allylic position and formation of alcohols. With an electron-rich double bond, the Paternó–Büchi products were isolated as well. The different diastereomers were separated by column chromatography or HPLC. Their relative configurations were determined using NOESY measurements or X-ray structure analysis. Overall, β-γ-unsaturated spirolactones show a remarkably different photochemistry compared to other cyclohexadienes, affording new products in only a few steps.

1. Introduction

The photochemistry of 1,4-cyclohexadiene (**1**) has been investigated in solution and in the gas phase [1–3]. More recently, a theoretical study highlighted the importance of conical intersections during irradiation at 185 nm [4]. The main products in the solution are bicyclo[3.1.0]hex-2-ene (**2**), 1,3-cyclohexadiene (**3**), and benzene (**4**) (Scheme 1).
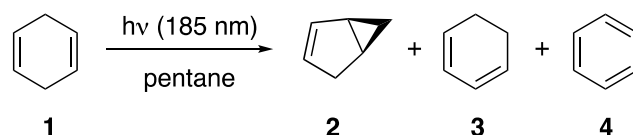
Scheme 1. Photochemistry of 1,4-cyclohexadiene (**1**).

The formation of bicyclic compound **2** is especially interesting from the mechanistic point of view because it results from a di-π-methane rearrangement. Such reactions were discovered by Zimmerman, who summarized the first examples in a review exactly 50 years ago [5] and with a focus on synthetic applications later on [6,7]. In contrast to 1,4-cyclohexadiene (**1**), 1,4-bridged systems like barrelene (**5**) or benzonorbornadiene (**6**) have the advantage that they cannot undergo double-bond migration or aromatization. Very recently, Bach showed that 2-azabarrrelenones (**7**) are efficient precursors for the di-π-methane rearrangement as well (Figure 1) [8].
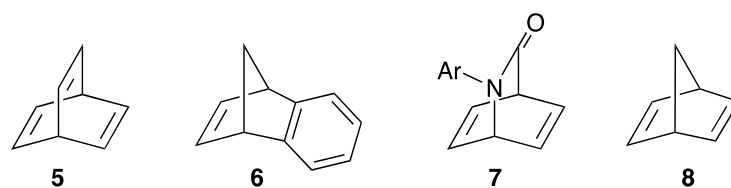
Figure 1. Suitable precursors for di-π-methane rearrangements or [2 + 2] photodimerizations.

Another important reaction pathway for alkenes under irradiation is the [2 + 2] photodimerization [9]. Such transformations can be performed under direct excitation or sensitization. Norbornadiene (**8**) represents a suitable precursor, which dimerizes under metal catalysis in the presence of copper, chromium, or nickel complexes [10–12]. The dihedral angle between the two double bonds fits well for metal coordination, which is not possible with 1,4-cyclohexadiene (**1**), as it prefers a more planar geometry [1].

During our studies on Birch reductions of aromatic carboxylic acids (**9**) [13–16], we developed an easy entry to γ-spirolactones **11** in the presence of ethylene oxide (**10**) (Scheme 2) [17]. The reactions can be performed on a large scale and the yields are high. Due to the quaternary spiro center, the products cannot split off hydrogen to form arenes, which is a problem with 1,4-cyclohexadiene (see Scheme 1). Therefore, we became interested in the photochemistry of such β-γ-unsaturated spirolactones **11**, without additives and in the presence of carbonyl compounds.
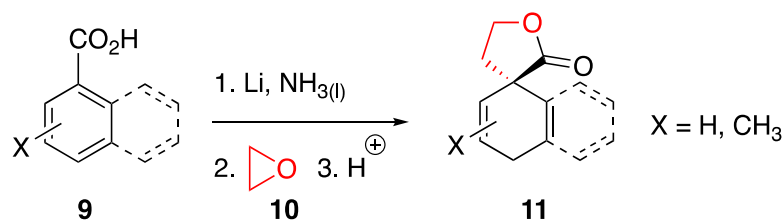
Scheme 2. Synthesis of β-γ-unsaturated spirolactones **11** by Birch reduction of aromatic carboxylic acids (**9**) in the presence of ethylene oxide (**10**).

2. Results and Discussion

2.1. Photochemistry of Sole β-γ-Unsaturated Spirolactones **11**

To find the proper conditions for photochemical reactions, we measured the UV spectra of β-γ-unsaturated spirolactone **11a** (X = H) and compared it with cyclohexadiene (**1**) and norbornadiene (**8**) (Figure 2). Interestingly, our compound **11a** shows a distinct absorption band at 230 nm, which is not present in the spectra of the other dienes. This can only be explained by the influence of the lactone group. Although the π-systems are not conjugated, an interaction through space might be possible [18]. To further elucidate this behavior, we calculated energies of the excited states of β-γ-unsaturated spirolactone **11a** on a TDDFT level (MN15/6-31G*). Indeed, we found a long-wave excited singlet state at 244.8 nm. A consideration of the six orbitals involved in this excitation (HOMO-2, HOMO-1, HOMO, LUMO, LUMO+1, LUMO+2) revealed that both the C-C double bonds and the ester group contribute to the electronic excitation (for details and orbital energies see Figure S1). To conclude the UV measurements and calculations, it should be possible to conduct photochemistry of spirolactones **11** at middle ultraviolet, which is not suitable for cyclohexadiene (**1**) or norbornadiene (**8**).

To optimize the conditions, we started our photochemical studies with β-γ-unsaturated spirolactone **11a** (Table 1). First, a 0.05 M solution of **11a** in methyl *tert*-butyl ether (MTBE), with dimethyl suberate as the internal standard, was irradiated with two UV-B lamps (mainly emitting at 320–360 nm [19]) to prove that no side reactions are possible. Indeed, after 6 h of irradiation, no conversion was observed (entry 1). However, after 24 h we saw a decrease of starting material and broad signals in the NMR of the crude product. That speaks to the formation of higher molecular weight products which were found in the mass

spectrum as well. Additionally, we were able to isolate one side product using column chromatography in a very low yield (entry 2). The structure was unequivocally assigned as ketone **12a** (Figure 3, Section 3). This can be explained by the auto-oxidation of the allylic position with traces of oxygen under irradiation. Indeed, when we bubbled oxygen through the solution, the amount of ketone **12a** increased to 8%, apart from more polymeric material (entry 3). On the other hand, in the dark or with careful exclusion of oxygen, no conversion was observed (entries 4 and 5). These results show that anaerobic conditions are important and that the allylic position is prone to hydrogen atom abstraction, leading to polymeric material. Thus, all subsequent reactions were carried out under careful exclusion of oxygen.
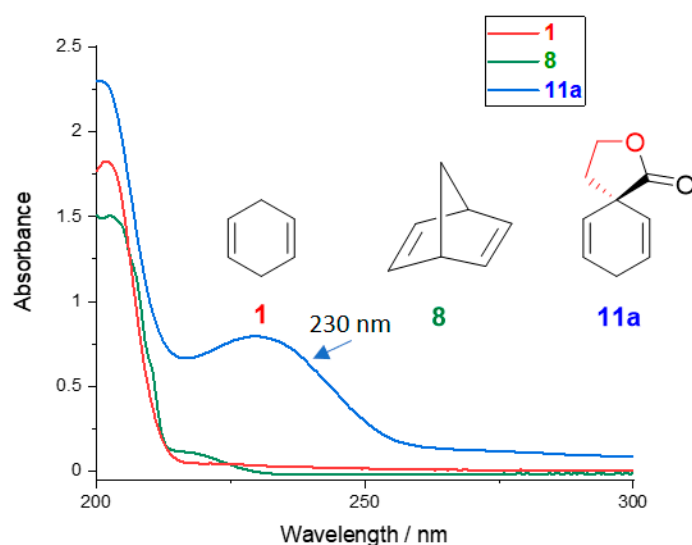

Figure 2. UV spectra of cyclohexadiene (**1**), norbornadiene (**8**) and spirolactone **11a**.

Table 1. Optimization of photochemical reactions of β-γ-unsaturated spirolactone **11a** [1].

Entry	Solvent	Light Source	Time (h)	Conv. (%) [2]	Additive	Product (%) [3]
1	MTBE	UV-B	6	<5	–	–
2	MTBE	UV-B	24	43	–	**12a** (3)
3	MTBE	UV-B	24	87	O_2 [4]	**12a** (8)
4	MTBE	–	24	<5	O_2 [4]	–
5	MTBE	UV-B	24	<5	– [5]	–
6	MTBE	Rayonet	6	10	–	–
7	MTBE	Rayonet	24	44	–	**13a** (6)
8	MTBE	Rayonet	120	86	–	**13a** (5)
9	MTBE	Rayonet	24	42	Cu(I)OTf [6]	–
10	MTBE	UV-C [7]	6	58	–	–
11	CH_3CN	UV-C [7]	12	90	–	**13a** (10)
12	acetone	UV-C [7]	12	12	–	–
13	CH_3CN	UV-B	12	<5	Xanthone	–
14	CH_3CN	UV-C [7]	12	88	Isoprene	**13a** (9)
15	CH_3CN [8]	UV-C [7]	5	93	–	**13a** (14)
16	CH_3CN	UV-C [7]	3	41	–	**13a** (18) [9]

[1] Spirolactone **11a** (600 mg, 4.0 mmol) and the internal standard dimethyl suberate (202 mg, 1.0 mmol) in the appropriate solvent (80 mL) were irradiated with the given light source. [2] Determined from the NMR spectra of crude products in relation to the internal standard. [3] Isolated products after column chromatography. [4] Bubbling of oxygen through the solution. [5] Careful exclusion of oxygen. [6] 0.1 equiv. of Cu(I)OTf. [7] Close proximity of sample and two UV-C lamps (for setup see Figure S4). [8] Reaction of spirolactone **11a** (60 mg, 0.4 mmol) in 80 mL of CH_3CN. [9] In total, 44% yield related to the conversion.
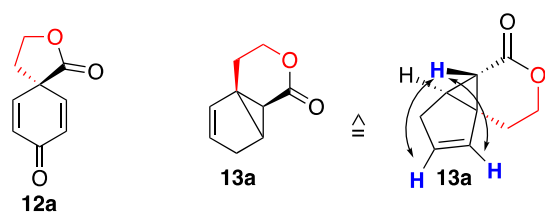
Figure 3. Isolated products **12a** and **13a** from photoreaction of spirolactone **11a**.

Next, we investigated reactions in a Rayonet reactor, fitted with 14 UV-C lamps. They are mainly emitting at 230–300 nm [19] and should be suitable to excite the absorption band at 230 nm (see Figure 2). However, after 6 h we observed only 10%, after 24 h, 44%, and after 5 d, 86% conversion (entries 6–8). The addition of copper(I) triflate, a suitable catalyst for [2 + 2] photodimerizations [9,12], did not accelerate the reaction (entry 9). We were able to isolate a new product **13a** in a very low yield. An explanation might be that the long distance between the sample and the light source in a Rayonet reactor, resulting in long reaction times. Therefore, we constructed our own photochemical setup, placing a quartz tube with the substrate in close proximity (5 cm) to two UV-C lamps (Figure S4). Under such conditions, the conversion was much higher after 6 h (entry 10). Another problem was the solubility of products in MTBE because we observed the deposition of material at the glass surface. Thus, we switched to acetonitrile as the solvent and obtained 90% conversion after 12 h of irradiation (entry 11). Although we saw broad signals in the NMR of the crude product, which speaks again for higher molecular weight material, we detected, apart from starting material **11a**, only one new product **13a**. The compound was isolated using column chromatography in a 10% yield in an analytically pure form (entry 11, for analytical data, see Section 3, for NMR spectra, see the Supplementary Materials). The structure elucidation of the new compound **13a** was not straightforward because it did not fit the expected products of [2 + 2] photodimerization or di-π-methane rearrangement. Thus, HRMS clearly showed a peak of [M + H]$^+$: 151.0733, exactly like the starting material, and a dimerization can be excluded. On the other hand, a di-π-methane rearrangement would fit with the HRMS, but it would afford various regio- and stereoisomers (see calculations in Figure 4). Interestingly, in our photoreaction, only one isomer is formed. After careful examination of 2D NMR spectra, including HSQC, HMBC, and NOESY, we determined a tricyclic compound **13a** as the most likely structure. Thus, no quaternary spiro carbon atom is detectable in the ^{13}C NMR spectrum. The proton alpha to the lactone ring and its NOE to the two vinylic protons are distinctive (Figure 3 and Supplementary Materials).
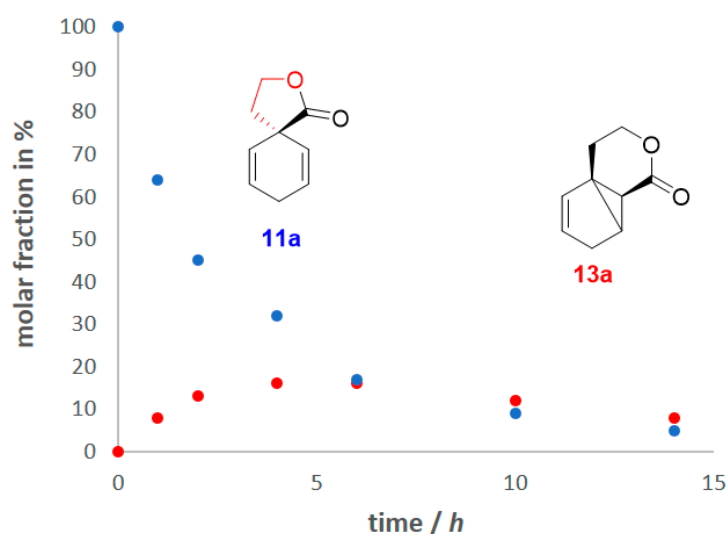

**Figure 4.** Kinetic measurement of the photoreaction of β-γ-unsaturated spirolactone **11a**.

The surprising formation of **13a** can only be explained by an oxa-di-π-methane rearrangement. Such reactions have been known for many years and interesting applications have been found with ketones and aldehydes [5,20]. However, to the best of our knowledge, only one example of an ester exists in the literature [21], oxa-di-π-methane rearrangements of lactones were hitherto unknown. We discuss the following mechanism depicted in Scheme 3.
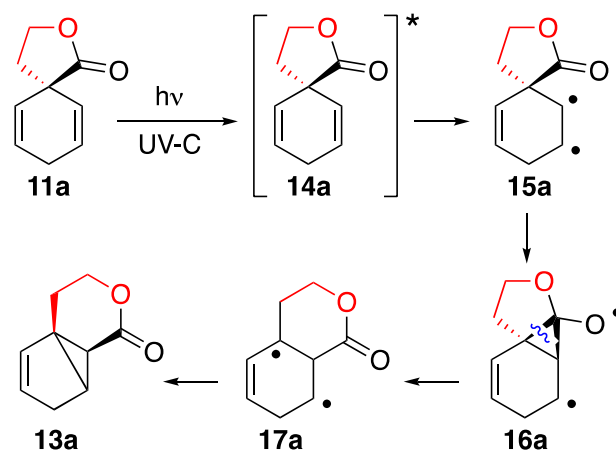
Scheme 3. Proposed mechanism for the formation of tricyclic compound **13a** from spirolactone (**11a**). * Represents the excited state.

After irradiation with UV-C light, an excited state **14a** is formed and diradical **15a** can attack the adjacent carbonyl group. Intermediate, **16a** should be short-lived and can react back or open to diradical **17a**, which finally affords the tricyclic compound **13a**. Interestingly, in contrast to di-π-methane rearrangements [7], almost all reactions of the oxa analogs have been discussed in the literature to proceed via their triplet states and, thus, sensitization was advantageous [5,20]. Therefore, we irradiated a solution of β-γ-unsaturated spirolactone **11a** in acetone with UV-C light for 12 h. However, we observed only a low conversion and no tricyclic compound **13a** could be detected in the NMR of the crude reaction mixture (Table 1, entry 12). The addition of xanthone, a suitable sensitizer for di-π-methane rearrangements [8], and irradiation at longer wavelengths gave no conversion either (entry 13). Finally, the addition of the known triplet quencher isoprene [22] did not inhibit the reaction (entry 14). All these results speak for a reaction from the excited singlet state, which was indeed postulated for the oxa-di-π-methane rearrangement of an ester [21].

To further prove our hypothesis, we performed DFT calculations of different reaction pathways for a di-π-methane rearrangement and the corresponding oxa analog in the photoreaction of β-γ-unsaturated spirolactone **11a** (Scheme 4). Starting with the excited spirolactone **11a**, five different biradicals (**BR1, BR2a,b**, and **BR3a,b**) are possible. **BR1** originates from the oxa-di-π-methane rearrangement while **BR2** and **BR3** are attributable to the di-π-methane rearrangement. The biradical **BR1** turns out to be not a stationary point at different levels of theory (B3LYP-D3/6-31G*, MN15/6-31G*, MN15/def2-TZVP) but immediately undergoes a ring opening to **BR4**. The relative energies of **BR4, BR2a,b**, and **BR3a,b** (referred to as **BR4** = 0.0 kcal/mol) are given in parentheses (Scheme 4). Out of these five biradicals, **BR4** is by far the most stable species. **BR4** exists in two resonance structures (due to the allyl radical moiety) and, therefore, two products (**P1** (= **13a**) and **P2**) would be possible. According to DFT calculations, **P1** is more stable than the most stable diastereomer of **P2** by 1.7 kcal/mol. It should be noted that **BR5** and **BR6** immediately undergo cyclization to **P3** and **P4** during calculation (for details of geometries and energies see Figures S2 and S3). In conclusion, our experimental and theoretical studies show that for spirolactone **11a**, the oxa-di-π-methane rearrangement is the preferred pathway, proceeding presumably via the singlet state.
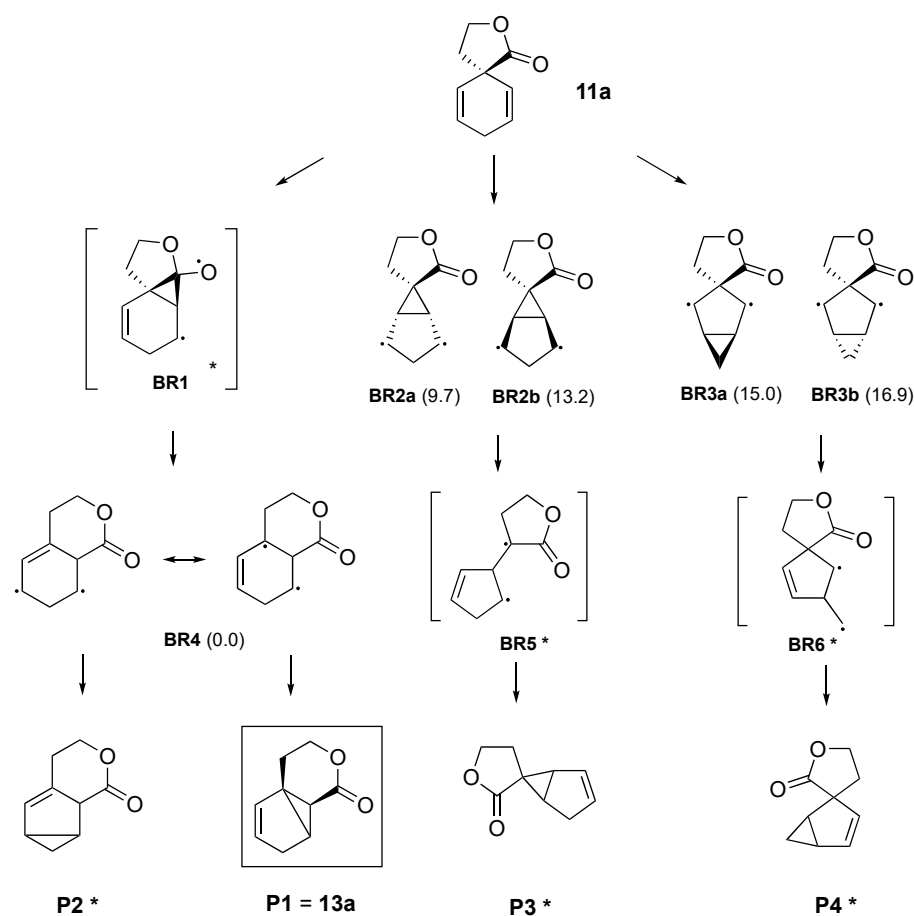
Scheme 4. Possible reaction pathways for photoreaction of β-γ-unsaturated spirolactone **11a** (* two diastereomers).

The main problem of the photochemistry of β-γ-unsaturated spirolactone **11a** is the formation of higher molecular weight material, with distinctive broad signals in the NMR spectra and many peaks in the mass spectra of the crude product. This can be explained by radical intermediates depicted in Scheme 3, which can undergo hydrogen atom abstraction at the allylic position and further additions to the double bonds of the starting material or product. Therefore, we irradiated higher diluted solutions, and the yield was slightly increased already after 5 h (Table 1, entry 15 vs. entry 11). However, because of the small scale, the total amount of tricyclic compound **13a** was very low. This problem might be resolved by continuous flow techniques in future work. To investigate the influence of the conversion on the yield, we conducted kinetic measurements with dimethyl suberate as the internal standard in deuterated acetonitrile (Figure 4, Section 3).

After 1 h, we see the conversion of 36% and the formation of 8% of product **13a**. After 2 h, 55% conv. and 13% of product. Thus, already after a short time, decomposition and formation of higher molecular weight material occurs. When we increased the irradiation time to 3, 4, and 6 h, the conversion was higher but the amount of product only slightly increased, and after 12 h we even saw a decrease in the yield of tricyclic compound **13a**, in accordance with the preparative reaction (entry 11). This speaks to a decomposition of this product under longer irradiation time. Indeed, after 24 h, only small amounts of product **13a** were left. Thus, it would be advantageous to stop the reaction at lower conversions because the starting material **11a** can be easily separated using column chromatography. We found the best conditions on a preparative scale with 3 h of irradiation. Thus, tricycle **13a** was isolated in an 18% absolute yield its an analytically pure form (entry 16, Section 3). Related to the conversion of 41%, the corrected yield is even higher (44%).

After optimization of the reaction conditions, we became interested in the photochemistry of other β-γ-unsaturated spirolactones **11**. We investigated dimethyl **11b** and naphthyl **11c** derivatives, both easily available through Birch reduction of the corresponding aromatic carboxylic acids in the presence of ethylene oxide [17], and compared it with lactone **11a** (Scheme 5). Again, we observe only the oxa-di-π-methane rearrangement, apart from the formation of higher molecular weight material, and it was advantageous to stop the reactions at lower conversions. Interestingly, dimethyl β-γ-unsaturated spirolactone **11b** affords two regioisomers (**13ba** and **13bb**) because both double bonds can be excited. On the other hand, in the naphthyl system **11c**, only one bond can react.
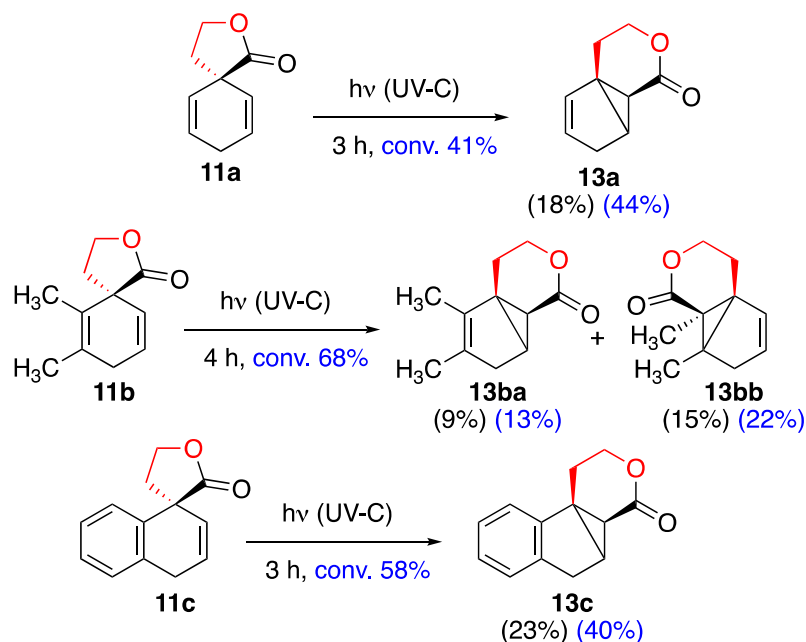
Scheme 5. Photoreaction of sole β-γ-unsaturated spirolactones **11**. Yields in blue are related to the conversion.

The lability of the starting materials and products leads to decomposition, and the yields are only moderate. But we were able to isolate all products using column chromatography or HPLC in pure forms (Section 3 and the Supplementary Materials). Furthermore, we obtained an X-ray structure of product **13c** as a final proof that an oxa-di-π-methane rearrangement occurs (Figure 5). To summarize the photochemistry of β-γ-unsaturated spirolactones **11**, they show an absorption band at 230 nm, which allows irradiations with UV-C light without additives. The reactions proceed presumably via the singlet excited state, affording only product **13** of an oxa-di-π-methane rearrangement. Although the yields are only moderate, because the compounds easily polymerize, we could synthesize interesting new lactones and elucidate the mechanism of their formation.
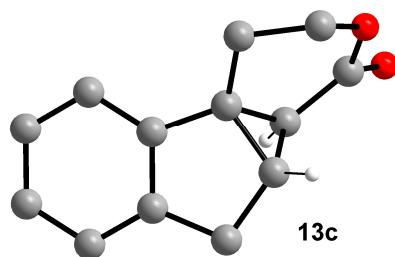

Figure 5. Crystal structure of product **13c**.

2.2. Photochemistry of β-γ-Unsaturated Spirolactones **11** *in the Presence of Carbonyl Compounds*

After the successful reactions of sole β-γ-unsaturated spirolactones **11**, we became interested in their photochemistry in the presence of carbonyl compounds. Such functional groups can undergo a [2 + 2] cycloaddition to alkenes, affording oxetanes, known for many years as the Paternó–Büchi reaction [23–25]. Electron-rich double bonds like enol ethers give high yields, but the addition of benzaldehyde (**18**) to cyclohexene has been described as well [26,27]. Already these studies showed that, apart from oxetane formation, hydrogen atom abstraction from the allylic position can compete. This pathway was predominant when 1,4-cyclohexadiene (**1**) was used as a precursor with benzophenone (**19**) as the carbonyl compound [28]. UV spectra of benzaldehyde (**18**) and benzophenone (**19**) indicated that their n-π*absorption bands can be excited with UV-B light, whereas spirolactone **11a** does not react (Figure 6).

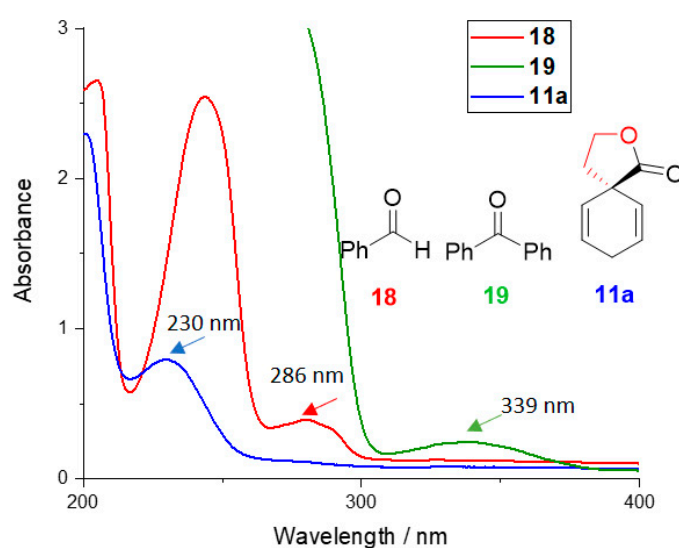**Figure 6.** UV spectra of benzaldehyde (**18**), benzophenone (**19**) and spirolactone **11a**.

Thus, we started our investigations with β-γ-unsaturated spirolactone **11a** and benzaldehyde (**18**). A 1:1 mixture was dissolved in acetonitrile in the presence of dimethyl suberate as a internal standard and irradiated with two UV-B lamps (Section 3). However, after 6 h, we observed only a 10% conversion and, therefore, we increased the time and equivalents of benzaldehyde (**18**). Indeed, now we obtained a 75% conversion and the allylic coupling product **20a** in a 32% yield (Scheme 6).

From the mechanistic point of view, benzaldehyde (**18**) forms triplet excited state **21** in the first step. This intermediate can abstract a hydrogen atom from the allylic position, affording radicals **22** and **23a**. Because the BDE of the CH bond is very low [29], oxetane formation cannot compete. Finally, recombination leads to the product **20a**, but other reaction pathways are possible as well (Scheme 6). Thus, dimerization of radical **22** affords hydrobenzoin (**24**) and additional hydrogen atom abstraction benzyl alcohol (**25**), both side products were isolated after column chromatography. Radical **23a** might add to the starting material, resulting in a higher molecular weight material as in photoreactions of sole spirolactone **11a** (Section 2.1). Indeed, we observed broad signals in the NMR spectra of the crude product, explaining the only moderate yield. The addition of six equiv. of benzaldehyde (**18**) and longer reaction times did not increase the yield because hydrogen atom abstraction from product **20a** is possible as well, resulting in decomposition. On the other hand, reducing the irradiation time to 6 h was advantageous and gave higher yields related to the conversion (Scheme 7).
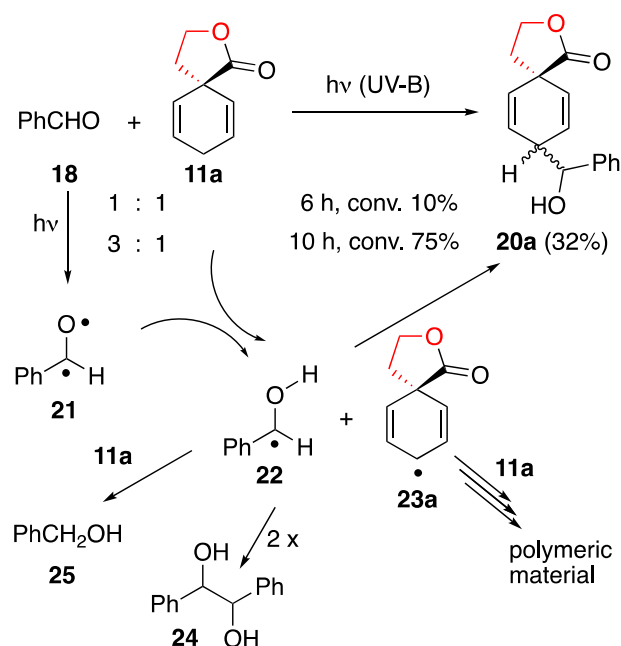
Scheme 6. Proposed mechanism for the photoreaction of β-γ-unsaturated spirolactone **11a** with benzaldehyde (**18**).
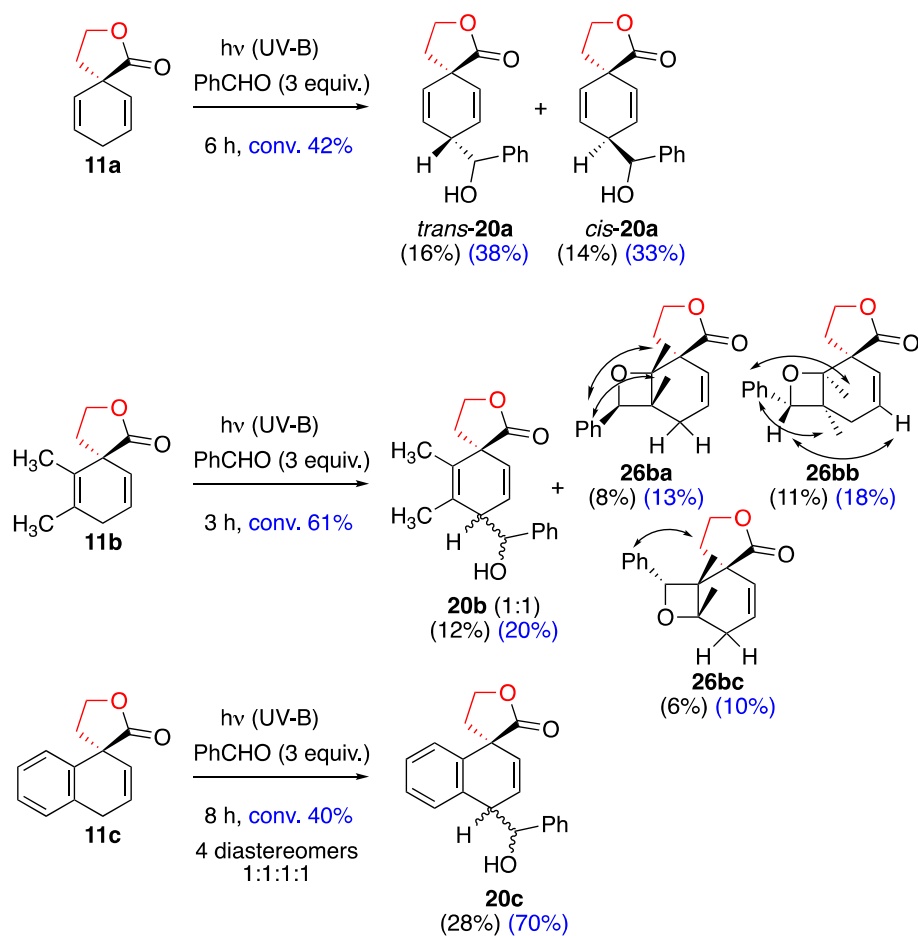
Scheme 7. Photoreaction of β-γ-unsaturated spirolactones **11** with benzaldehyde (**18**). Yields in blue are related to the conversion.

Interestingly, we obtained only two *cis/trans* diastereomers **20a** in a ratio of almost 1:1 because no stereogenic center is generated at the benzylic position. We were able to separate these isomers using column chromatography and isolated the products in an analytically pure form (Section 3 and the Supplementary Materials). Furthermore, we could assign the *trans* isomer unequivocally using NOESY measurements with a distinctive effect between the benzylic proton and the lactone CH$_2$ group (Figure 7 and the Supplementary Materials).
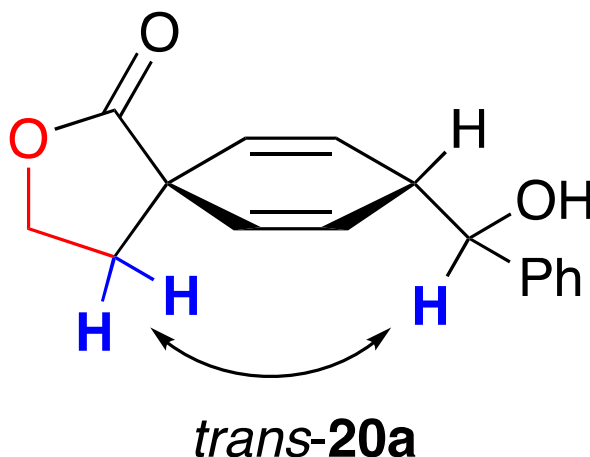

Figure 7. Distinctive NOESY interaction in product *trans*-**20a**.

After the successful reaction of spirolactone **11a** with benzaldehyde (**18**), we applied our optimized conditions to dimethyl **11b** and naphthyl **11c** derivatives as well (Scheme 7). Again, it was advantageous to stop the reactions after shorter irradiation times, resulting in higher yields related to the conversions. In contrast to spirolactone **11a**, the derivative **11b** showed a complex NMR of the crude product, due to the formation of various diastereomers **20b**. Furthermore, we observed for the first time Paternó–Büchi products **26b** as well. This can be explained by the electron-rich double bond with two methyl groups, which is more reactive [23–25]. We were able to isolate five products in almost pure form and assigned their relative configurations using NOESY measurements. Finally, the naphthyl derivative **11c** afforded all four possible allylic products **20c** in almost equal amounts, which were separated by column chromatography and HPLC (Section 3 and the Supplementary Materials).

To overcome the problem of complex diastereomeric mixtures, we finally became interested in the photochemical addition of benzophenone (**19**) to β-γ-unsaturated spirolactones **11**. Now all reactions afford only *cis/trans* isomers **27**, which were isolated in moderate yields (Scheme 8). Furthermore, the stereoselectivities are higher, which can be explained by the high steric demand of the benzophenone moiety. For the same reasons, the dimethyl derivative **11b** does not undergo a Paternó–Büchi reaction with benzophenone (**19**) in contrast to benzaldehyde (**18**) (Scheme 7). We were able to isolate all products using direct crystallization or column chromatography in a pure form (Section 3 and the Supplementary Materials). The *cis/trans* configuration was assigned using NOESY measurements and distinctive interactions of the aryl group with the methylene group of the lactone ring for the *trans*-isomers. Furthermore, we obtained single crystals from alcohols *cis*-**27a**, *trans*-**27b**, and *trans*-**27c**, and could unequivocally assign their relative configurations using X-ray structures (Figure 8, for details see the Supplementary Materials).
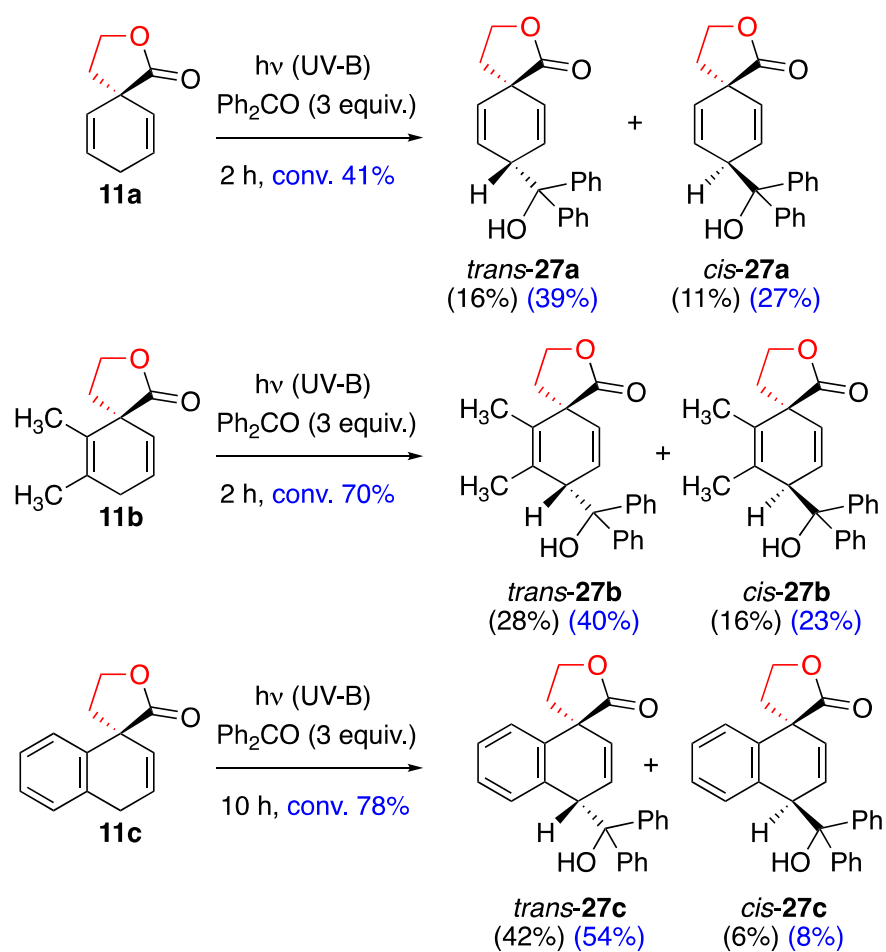
Scheme 8. Photoreaction of β-γ-unsaturated spirolactones **11** with benzophenone (**19**). Yields in blue are related to the conversion.
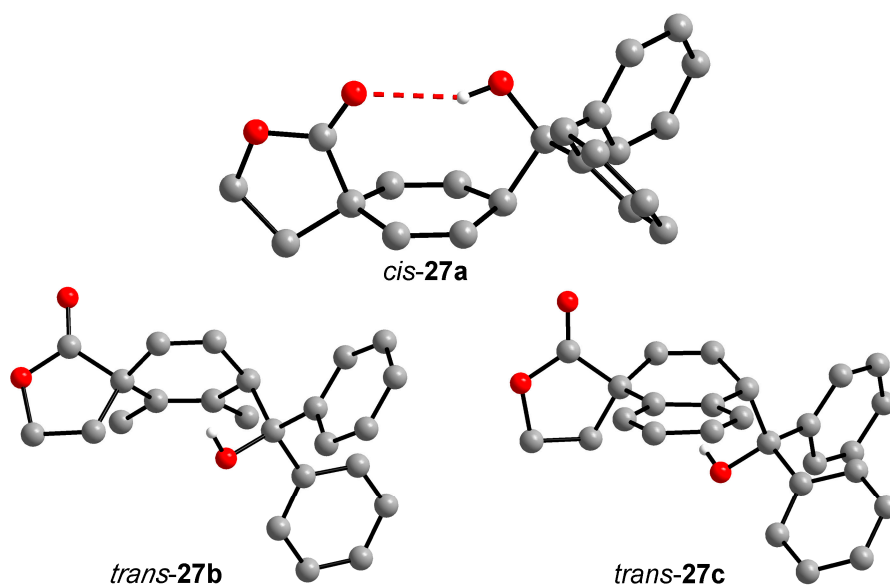

Figure 8. Crystal structures of products *cis*-**27a**, *trans*-**27b**, and *trans*-**27c**.

3. Materials and Methods

3.1. Chemicals and Instrumentation

First irradiations were performed with a Rayonet reactor, equipped with 14 UV-C lamps. After optimization of the conditions (Table 1), we constructed our own photochemical setup (Figure S4). Two UV-B lamps (Phillips UV-B PL-L 36 W, mainly emitting at 320–360 nm) or two UV-C lamps (Osram Puritec UVC HNS L60 W, mainly emitting at 230–300 nm) were used. Irradiations were performed in 100 mL quartz tubes, which were brought under argon atmosphere and sealed from air. The distance between the lamps and the reaction vessels was 5 cm (for the setup see Figure S4). MTBE or acetonitrile gradient grade > 99.9% was used as a solvent for irradiation. UV/vis spectra were measured with a UNICAM 3 spectrometer.

Melting points were determined by using a Mel-Temp from Electrothermal. TLC was performed using TLC silica gel 60 F254 aluminum sheets from Merck. For column chromatography, methyl *tert*-butyl ether (MTBE) and petrol ether (PE) in analytical grade were used. Preparative HPLC was performed on a Waters Delta Prep 4000 equipped with a UV/vis absorbance detector. A Prontosil 120-10-Si column was used with the dimension 250 × 20 mm. ^{1}H NMR and ^{13}C NMR spectra were measured by using a Bruker Avance NEO 500 (500 MHz, 125 MHz) or a Bruker Avance III 600 (600 MHz, 150 MHz) NMR spectrometer (we thank Angela Krtitschka for measuring the NMR spectra). Signals were assigned using two-dimensional methods (HSQC, HMBC, NOESY). IR spectra were recorded as a film by using a Nicolet Avatar 6700 FTIR spectrometer from Thermo Electron Corporation. High-resolution mass spectra (HRMS) were obtained using different spectrometers: ESI-Q-TOFmicro (Quadrupole-Time of Flight) Micromass Waters Inc. UK; LC-ESI-Q-TOF (Quadrupole-Time of Flight) maXis, Bruker Daltonics GmbH & Co. KG, Bremen, Germany; LC-ESI-Q-IM-TOF (Quadrupole-Ion mobility-Time of Flight) TimsTOF Pro2, Bruker Daltonics GmbH & Co. KG Bremen, Germany.

The crystal structures of the compounds **13c**, *cis*-**27a**, *trans*-**27b**, and *trans*-**27c** were determined using single crystal structure analysis. The data (**13c**: CCCD 2287188, *cis*-**27a**: CCDC 2287189, *trans*-**27b:** CCDC 2287193, *trans*-**27c**: CCDC 2287194) can be obtained free of charge from The Cambridge Crystallographic Data Centre, http://www.ccdc.cam.ac.uk (for details see the Supplementary Materials).

3.2. Photochemistry of Sole Spirolactones **11**

3.2.1. Kinetic Measurements

Spirolactone **11a** (30 mg, 0.2 mmol) and the internal standard octandioic acid dimethyl ester (dimethyl suberate) (20 mg, 0.1 mmol) were dissolved in deuterated acetonitrile (4 mL) in a 10 mL quartz tube. Prior to irradiation, the first ^{1}H NMR spectrum was taken ($t = 0$). Then, the sample was irradiated with UV-C light as described above, and the ^{1}H NMR spectra were recorded after constant time intervals. Irradiation was interrupted until the NMR sample was transferred back to the tube.

3.2.2. Analytical Data of Side Product 2-Oxaspiro[4.5]deca-6,9-diene-1,8-dione (**12a**)

Obtained as a colorless liquid. R_f = 0.13 (PE/MTBE 2:1). ^{1}H NMR (500 MHz, CDCl$_3$): δ = 2.63 (t, J = 6.9 Hz, 2H), 4.60 (t, J = 6.9 Hz, 2H), 6.51 (d, J = 10.1 Hz, 2H), 6.86 (d, J = 10.1 Hz, 2H). ^{13}C NMR (125 MHz, CDCl$_3$): δ = 34.6 (t), 49.6 (s), 65.7 (t), 131. 7 (d), 143.3 (d), 172.1 (s), 184.4 (s). IR (neat): ν = 2972, 2925, 1746, 1659, 1624, 1450, 1376, 1149, 1018, 863, 766 cm^{-1}. HRMS (ESI-Q-TOF): m/z Calcd for C$_9$H$_9$O$_3$ [M + H]$^+$: 165.0552; Found: 165.0547.

3.2.3. Optimized Procedure for Oxa-Di-π-Methane Rearrangements of Spirolactones **11**

Spirolactone **11** (4.0 mmol) and the internal standard octandioic acid dimethyl ester (dimethyl suberate) (202 mg, 1.0 mmol) were dissolved in 80 mL of acetonitrile and irradiated with UV-C light by the above-described procedure within appropriate time intervals (3 h for spirolactones **11a** and **11c**, 4 h for **11b**). Thereafter, a sample (4 mL) was taken, the solvent evaporated, the sample re-dissolved in CDCl$_3$, and a ^{1}H NMR spectrum was

measured to determine the conversion. Finally, all solvent was removed by evaporation, and the crude product was dissolved in MTBE and passed through a short silica gel plug. The silica gel was washed thoroughly with MTBE until no further product material was detected by TLC. Then, higher molecular weight material, which was stuck on the silica, was washed off with acetone (100 mL) and MeOH (100 mL). The MTBE solution, containing the product, internal standard, and starting material together with small amounts of higher molecular weight material, was evaporated and the residue was purified by column chromatography using MTBE/PE (1:2). The internal standard and starting material **11** were obtained first, followed by the products **13,** and finally small amounts of higher molecular weight material.

3.2.4. Analytical Data of Oxa-Di-π-Methane Rearrangement Products **13**

1,2,4b,5-tetrahydrocyclopenta[2,3]cyclopropa[1,2-c]pyran-4(4aH)-one (**13a**): Obtained as a colorless liquid. R_f = 0.21 (PE/MTBE 2:1). ^{1}H NMR (500 MHz, CDCl$_3$): δ = 1.33 (d, J = 2.9 Hz, 1H), 2.10 (ddd, J = 13.9, 3.5, 1.4 Hz, 1H), 2.44 (ddd, J = 13.9, 13.2, 5.8 Hz, 1H), 2.50 (dd, J = 6.9, 2.9 Hz, 1H), 2.55 (dt, J = 18.9, 2.2 Hz, 1H), 2.79 (ddt, J = 18.9, 6.9, 2.2 Hz, 1H), 4.10 (ddd, J = 13.2, 11.8, 3.5 Hz, 1H), 4.36 (ddd, J = 11.8, 5.8, 1.4 Hz, 1H), 5.61 (dt, J = 5.6, 2.2 Hz, 1H), 5.92 (dt, J = 5.6, 2.2 Hz, 1H). ^{13}C NMR (125 MHz, CDCl$_3$): δ = 22.0 (t), 25.8 (d), 32.6 (d), 36.3 (t), 40.8 (s), 66.1 (t), 130.0 (d), 133.9 (d), 171.1 (s). IR (neat): ν = 2922, 1716, 1451, 1396, 1267, 1158, 1024, 912, 864 cm^{-1}. HRMS (ESI-Q-TOF): m/z Calcd for C$_9$H$_{11}$O$_2$ [M + H]$^+$: 151.0759; Found: 151.0733.

4a,4b-dimethyl-1,2,4b,5-tetrahydrocyclopenta[2,3]cyclopropa[1,2-c]pyran-4(4aH)-one (**13ba**): Obtained as a colorless liquid. R_f = 0.29 (PE/MTBE 2:1). ^{1}H NMR (500 MHz, CDCl$_3$): δ = 1.27 (s, 1H), 1.57 (sext, J = 1.1 Hz, 3H), 1.67 (ddq, J = 2.6, 1.6, 1.1 Hz, 3H), 1.96 (ddd, J = 13.8, 3.5, 1.4 Hz, 1H), 2.33 (ddd, J = 13.8, 13.2, 5.8 Hz, 1H), 2.34 (ddqq, J = 18.0, 2.8, 1.6, 1.1 Hz, 1H), 2.40 (dd, J = 6.7, 2.8 Hz, 2H), 2.65 (ddqq, J = 18.0, 6.7, 2.6, 1.1 Hz, 1H), 4.07 (ddd, J = 13.2, 11.7, 3.5 Hz, 1H), 4.33 (ddd, J = 11.7, 5.8, 1.4 Hz, 1H). ^{13}C NMR (125 MHz, CDCl$_3$): δ = 11.0 (q), 13.5 (q), 21.2 (t), 24.8 (d), 32.8 (d), 40.0 (t), 43.0 (s), 65.8 (t), 131.2 (s), 133.0 (s), 171.6 (s). IR (neat): ν = 2970, 2924, 1716, 1387, 1291, 1157, 1108, 1038, 779 cm^{-1}. HRMS (ESI-Q-TOF): m/z Calcd for C$_{11}$H$_{15}$O$_2$ [M + H]$^+$: 179.1072; Found: 179.1053.

6,7-dimethyl-1,2,4b,5-tetrahydrocyclopenta[2,3]cyclopropa[1,2-c]pyran-4(4aH)-one (**13bb**): Obtained as a colorless liquid. R_f = 0.24 (PE/MTBE 2:1). ^{1}H NMR (500 MHz, CDCl$_3$): δ = 1.11 (s, 3H), 1.20 (s, 3H), 2.08 (ddd, J = 15.2, 11.5, 5.5 Hz, 1H), 2.17 (ddd, J = 15.2, 3.7, 2.7 Hz, 1H), 2.42 (t, J = 2.1 Hz, 2H), 4.21 (ddd, J = 11.5, 10.9, 3.7 Hz, 1H), 4.26 (ddd, J = 10.9, 5.5, 2.7 Hz, 1H), 5.63 (dt, J = 5.7, 2.1 Hz, 1H), 5.67 (dt, J = 5.7, 2.1 Hz, 1H). ^{13}C NMR (125 MHz, CDCl$_3$): δ = 9.3 (q), 15.8 (q), 23.2 (t), 28.7 (s), 35.9 (s), 40.8 (t), 43.1 (s), 67.6 (t), 131.2 (d), 133.0 (d), 174.2 (s). IR (neat): ν = 2974, 2917, 1711, 1402, 1253, 1221, 1071, 937, 732 cm^{-1}. HRMS (ESI-Q-TOF): m/z Calcd for C$_{11}$H$_{15}$O$_2$ [M + H]$^+$: 179.1072; Found: 179.1049.

1,2,4b,5-tetrahydroindeno[1′,2′:2,3]cyclopropa[1,2-c]pyran-4(4aH)-one (**13c**): Obtained as a white solid. Mp = 54–56 °C. R_f = 0.26 (PE/MTBE 2:1). ^{1}H NMR (500 MHz, CDCl$_3$): δ = 1.49 (d, J = 3.0 Hz, 1H), 2.26 (dd, J = 13.8, 3.4 Hz, 1H), 2.78 (ddd, J = 13.8, 13.3, 5.8 Hz, 1H), 2.80 (dd, J = 6.5, 3.0 Hz, 1H), 3.12 (d, J = 17.7 Hz, 1H), 3.31 (dd, J = 17.7, 6.5 Hz, 1H), 4.24 (ddd, J = 13.3, 11.8, 3.4 Hz, 1H), 4.47 (dd, J = 11.8, 5.8 Hz, 1H), 7.21–7.30 (m, 4H). ^{13}C NMR (125 MHz, CDCl$_3$): δ = 21.0 (t), 26.6 (d), 32.9 (d), 34.7 (t), 39.4 (s), 65.7 (t), 121.9 (d), 125.7 (d), 126.7 (d), 127.2 (d), 141.0 (s), 143.9 (s), 170.2 (s). IR (neat): ν = 2969, 2916, 1713, 1479, 1399, 1247, 1218, 1077, 1022, 937, 807, 754 cm^{-1}. HRMS (ESI-Q-TOF): m/z Calcd for C$_{13}$H$_{13}$O$_2$ [M + H]$^+$: 201.0916; Found: 201.0904.

3.3. Photochemistry of Spirolactones **11** *in the Presence of Carbonyl Compounds*
3.3.1. Optimized Procedure for Reactions with Benzaldehyde (**18**) or Benzophenone (**19**)

Spirolactone **11** (4.0 mmol), benzaldehyde (**18**) (1.26 g, 12.0 mmol) or benzophenone (**19**) (2.19 g, 12.0 mmol), and the internal standard octandioic acid dimethyl ester (dimethyl

suberate) (202 mg, 1 mmol) were dissolved in 80 mL of acetonitrile and irradiated with UV-B light for 2–10 h. Thereafter, a sample (4 mL) was taken, the solvent evaporated, the sample re-dissolved in $CDCl_3$, and a ^1H NMR spectrum was measured to determine the conversion. The solvent was removed by evaporation and the crude product was purified by column chromatography using MTBE/PE 1:1 as the eluent. In some cases, the desired product precipitated directly and could be isolated by filtration.

The unreacted carbonyl compound and the internal standard were eluted first, followed by side products like benzyl alcohol (**25**) and hydrobenzoin (**24**). The products **20** and **26** were obtained next, in yields given in Schemes 7 and 8. Finally, the solvent was switched to acetone and higher molecular weight material was found in the last fractions. Diastereomers **20**, **26**, and **27** were separated by a second column or HPLC and were isolated in pure form (Supplementary Materials).

3.3.2. Analytical Data of Products **20** and **26** from Reactions with Benzaldehyde (**18**)

trans-8-[hydroxy(phenyl)methyl]-2-oxaspiro[4.5]deca-6,9-dien-1-one (*trans-***20a**): Obtained as a colorless liquid. R_f = 0.10 (PE/MTBE 2:1). ^1H NMR (500 MHz, $CDCl_3$): δ = 1.98 (bs, 1H), 2.06 (t, J = 7.0 Hz, 2H), 3.37 (dtt, J = 5.2, 3.2, 2.0 Hz, 1H), 4.34 (t, J = 7.0 Hz, 2H), 4.79 (d, J = 5.2 Hz, 1H), 5.72 (dd, J = 10.3, 2.0 Hz, 1H), 5.74 (dd, J = 10.1, 2.0 Hz, 1H), 5.98 (ddd, J = 10.1, 3.2, 1.3 Hz, 1H), 5.99 (ddd, J = 10.3, 3.2, 1.3 Hz, 1H), 7.28–7.35 (m, 5H). ^{13}C NMR (125 MHz, $CDCl_3$): δ = 37.4 (t), 43.4 (d), 45.9 (s), 65.3 (t), 76.2 (d), 126.2 (d), 126.3 (d), 126.5 (d), 126.8 (d), 127.8 (d), 128.1 (d), 129.0 (d), 141.4 (s), 177.5 (s). IR (neat): ν = 3664, 3458, 2969, 2919, 1749, 1450, 1374, 1205, 1165, 1021, 914, 852, 766 cm^{-1}. HRMS (ESI-Q-TOF): m/z Calcd for $C_{16}H_{17}O_3$ [M + H]$^+$: 257.1178; Found: 257.1186.

cis-8-[hydroxy(phenyl)methyl]-2-oxaspiro[4.5]deca-6,9-dien-1-one (*cis-***20a**): Obtained as a colorless liquid. R_f = 0.12 (PE/MTBE 2:1). ^1H NMR (500 MHz, $CDCl_3$): δ = 1.65 (bs, 1H), 2.39 (t, J = 7.0 Hz, 2H), 3.31 (dtt, J = 4.1, 3.8, 1.2 Hz, 1H), 4.48 (t, J = 7.0 Hz, 2H), 4.89 (d, J = 3.8 Hz, 1H), 5.73 (ddd, J = 9.9, 3.8, 1.5 Hz, 1H), 5.77 (ddd, J = 9.9, 2.0, 1.2 Hz, 1H), 5.80 (ddd, J = 9.8, 2.0, 1.2 Hz, 1H), 6.06 (ddd, J = 9.8, 4.1, 1.5 Hz, 1H), 7.27–7.39 (m, 5H). ^{13}C NMR (125 MHz, $CDCl_3$): δ = 36.6 (t), 44.8 (d), 46.6 (s), 65.7 (t), 74.4 (d), 126.0 (d), 127.1 (d), 127.2 (d), 127.3 (d), 127.6 (d), 128.2 (d), 130.3 (d), 142.7 (s), 178.8 (s). IR (neat): ν = 3454, 3029, 2915, 1751, 1373, 1205, 1166, 1021, 913, 851 cm^{-1}. HRMS (ESI-Q-TOF): m/z Calcd for $C_{16}H_{17}O_3$ [M + H]$^+$: 257.1178; Found: 257.1182.

trans-8-[hydroxy(phenyl)methyl]-6,7-dimethyl-2-oxaspiro[4.5]deca-6,9-dien-1-one (*trans-***20b**): Obtained as a colorless liquid. R_f = 0.16 (PE/MTBE 2:1). ^1H NMR (500 MHz, $CDCl_3$): δ = 1.62 (bs, 1H), 1.78 (s, 3H), 1.99 (s, 3H), 2.19 (ddd, J = 13.4, 7.7, 4.3 Hz, 1H), 2.78 (ddd, J = 13.4, 9.0, 8.3 Hz, 1H), 3.14–3.16 (m, 1H), 4.47 (ddd, J = 9.3, 8.3, 7.7 Hz, 1H), 4.51 (ddd, J = 9.3, 9.0, 4.3 Hz, 1H), 5.12 (d, J = 2.7 Hz, 1H), 5.46 (dd, J = 9.9, 4.4 Hz, 1H), 5.74 (dd, J = 9.9, 1.2 Hz, 1H), 7.25–7.38 (m, 5H). ^{13}C NMR (125 MHz, $CDCl_3$): δ = 15.7 (q), 17.8 (q), 33.4 (t), 50.7 (s), 51.1 (d), 66.2 (t), 71.3 (d), 125.8 (d), 126.0 (d), 126.6 (s), 126.9 (s), 127.4 (d), 128.1 (d), 128.3 (d), 143.2 (s), 180.2 (s). IR (neat): ν = 3413, 3030, 2914, 1758, 1451, 1378, 1202, 1170, 1024, 847, 760 cm^{-1}. HRMS (ESI-Q-TOF): m/z Calcd for $C_{18}H_{19}O_2$ [M − H_2O + H]$^+$: 267.1385; Found: 267.1399.

cis-8-[hydroxy(phenyl)methyl]-6,7-dimethyl-2-oxaspiro[4.5]deca-6,9-dien-1-one (*cis-***20b**): Obtained as a colorless liquid. R_f = 0.08 (PE/MTBE 2:1). ^1H NMR (500 MHz, $CDCl_3$): δ = 1.75 (bs, 1H), 1.78 (s, 3H), 1.96 (s, 3H), 2.10 (ddd, J = 13.1, 7.0, 3.3 Hz, 1H), 2.54 (dt, J = 13.1, 9.3 Hz, 1H), 3.14–3.17 (m, 1H), 4.38 (td, J = 9.3, 7.0 Hz, 1H), 4.42 (td, J = 9.3, 3.3 Hz, 1H), 5.05 (d, J = 2.9 Hz, 1H), 5.54 (dd, J = 10.0, 4.2 Hz, 1H), 5.88 (dd, J = 10.0, 1.3 Hz, 1H), 7.30–7.40 (m, 5H). ^{13}C NMR (125 MHz, $CDCl_3$): δ = 15.5 (q), 17.9 (q), 36.1 (t), 50.2 (d), 50.6 (s), 65.5 (t), 72.7 (d), 125.7 (d), 126.0 (d), 127.3 (d), 127.4 (s), 127.8 (d), 128.2 (d), 130.0 (s), 141.8 (s), 178.0 (s). IR (neat): ν = 3434, 3031, 2919, 1757, 1450, 1376, 1206, 1172, 1025, 912, 729 cm^{-1}. HRMS (ESI-Q-TOF): m/z Calcd for $C_{18}H_{19}O_2$ [M − H_2O + H]$^+$: 267.1390; Found: 267.1399.

1,6-dimethyl-7-phenylspiro[8-oxabicyclo[4.2.0]oct-3-ene-2,3′-oxolan]-2′-one (**26ba**): Obtained as a colorless liquid. R_f = 0.30 (PE/MTBE 2:1). ^{1}H NMR (500 MHz, CDCl$_3$): δ = 0.87 (s, 3H), 1.54 (s, 3H), 2.23 (dd, *J* = 16.7, 7.4 Hz, 1H), 2.29 (ddd, *J* = 13.5, 6.7, 4.0 Hz, 1H), 2.68 (ddd, *J* = 16.7, 3.3, 2.2 Hz, 1H), 2.73 (dt, *J* = 13.5, 9.3 Hz, 1H), 4.43–4.47 (m, 2H), 5.28 (s, 1H), 5.99 (dd, *J* = 9.6, 3.3 Hz, 1H), 6.39 (ddd, *J* = 9.6, 7.4, 2.2 Hz, 1H), 7.26–7.40 (m, 5H). ^{13}C NMR (125 MHz, CDCl$_3$): bδ = 19.4 (q), 20.2 (q), 31.7 (t), 36.2 (t), 44.0 (s), 54.0 (s), 66.1 (t), 86.7 (d), 88.7 (s), 125.0 (d), 127.3 (d), 128.2 (d), 129.5 (d), 132.9 (d), 140.7 (s), 177.4 (s). IR (neat): ν = 2993, 2917, 1758, 1450, 1377, 1205, 1168, 1023, 848, 760 cm^{-1}. HRMS (ESI-Q-TOF): *m/z* Calcd for C$_{18}$H$_{21}$O$_3$ [M + H]$^+$: 285.1491; Found: 285.1498.

1,6-dimethyl-7-phenylspiro[8-oxabicyclo[4.2.0]oct-3-ene-2,3′-oxolan]-2′-one (**26bb**): Obtained as a colorless liquid. R_f = 0.18 (PE/MTBE 2:1). ^{1}H NMR (500 MHz, CDCl$_3$): δ = 0.88 (s, 3H), 1.48 (s, 3H), 2.16 (ddd, *J* = 13.3, 9.1, 7.1 Hz, 1H), 2.19 (ddd, *J* = 16.8, 3.3, 2.2 Hz, 1H), 2.49 (ddd, *J* = 13.3, 8.3, 5.1 Hz, 1H), 2.56 (dd, *J* = 16.8, 7.1 Hz, 1H), 4.21 (ddd, *J* = 9.1, 8.3, 7.1 Hz, 1H), 4.36 (td, *J* = 9.1, 5.1 Hz, 1H), 5.93 (s, 1H), 6.31 (ddd, *J* = 9.5, 7.1, 2.2 Hz, 1H), 6.40 (dd, *J* = 9.5, 3.3 Hz, 1H), 7.26 (tm, *J* = 7.3 Hz, 1H), 7.35 (tm, *J* = 7.3 Hz, 2H), 7.53 (dm, *J* = 7.3 Hz, 2H). ^{13}C NMR (125 MHz, CDCl$_3$): δ = 14.4 (q), 25.4 (q), 31.8 (t), 37.9 (t), 49.5 (s), 50.5 (s), 66.1 (t), 83.7 (d), 85.0 (s), 126.3 (d), 127.1 (d), 128.0 (d), 129.4 (d), 132.9 (d), 140.8 (s), 179.8 (s). IR (neat): ν = 3028, 2918, 1750, 1377, 1173, 1024, 911, 837 cm^{-1}. HRMS (ESI-Q-TOF): *m/z* Calcd for C$_{18}$H$_{21}$O$_3$ [M + H]$^+$: 285.1491; Found: 285.1484.

1,6-dimethyl-8-phenylspiro[7-oxabicyclo[4.2.0]oct-3-ene-2,3′-oxolan]-2′-one (**26bc**): Obtained as a colorless liquid. R_f = 0.40 (PE/MTBE 2:1). ^{1}H NMR (500 MHz, CDCl$_3$): δ = 0.80 (ddd, *J* = 13.2, 6.5, 1.1 Hz, 1H), 1.53 (s, 3H), 1.77 (s, 3H), 1.96 (ddd, *J* = 13.2, 11.1, 9.3 Hz, 1H), 2.46 (dd, *J* = 17.1, 7.2 Hz, 1H), 2.73 (ddd, *J* = 17.1, 3.3, 2.2 Hz, 1H), 3.98 (ddd, *J* = 11.1, 9.3, 6.5 Hz, 1H), 4.15 (td, *J* = 9.3, 1.1 Hz, 1H), 5.44 (dd, *J* = 9.6, 3.3 Hz, 1H), 5.50 (s, 1H), 6.20 (ddd, *J* = 9.6, 7.2, 2.2 Hz, 1H), 7.27–7.35 (m, 5H). ^{13}C NMR (125 MHz, CDCl$_3$): δ = 19.2 (q), 24.7 (q), 31.3 (t), 39.0 (t), 50.1 (s), 51.6 (s), 65.5 (t), 85.4 (s), 86.8 (d), 127.6 (d), 127.8 (d), 127.9 (d), 128.0 (d), 133.0 (d), 138.6 (s), 177.8 (s). IR (neat): ν = 2988, 2919, 1751, 1450, 1377, 1173, 1024, 842, 752 cm^{-1}. HRMS (ESI-Q-TOF): *m/z* Calcd for C$_{18}$H$_{21}$O$_3$ [M + H]$^+$: 285.1491; Found: 285.1485.

4-[hydroxy(phenyl)methyl]-4H-spiro[naphthalene-1,3′-oxolan]-2′-one (**20c**) **DS1**: Obtained as a white solid. Mp = 65–66 °C. R_f = 0.24 (PE/MTBE 2:1). ^{1}H NMR (500 MHz, CDCl$_3$): δ = 2.15 (ddd, *J* = 13.2, 7.2, 5.7 Hz, 1H), 2.21 (ddd, *J* = 13.2, 7.8, 7.6 Hz, 1H), 2.80 (bs, 1H), 3.89 (ddd, *J* = 4.4, 3.7, 1.0 Hz, 1H), 4.40 (ddd, *J* = 9.2, 7.8, 5.7 Hz, 1H), 4.42 (ddd, *J* = 9.2, 7.6, 7.2 Hz, 1H), 5.11 (d, *J* = 3.7 Hz, 1H), 5.92 (dd, *J* = 10.0, 4.4 Hz, 1H), 5.97 (dd, *J* = 10.0, 1.0 Hz, 1H), 7.05–7.09 (m, 1H), 7.20–7.30 (m, 7H), 7.55–7.58 (m, 1H). ^{13}C NMR (125 MHz, CDCl$_3$): δ = 40.3 (t), 47.8 (d), 48.9 (s), 65.1 (t), 77.2 (d), 126.5 (d), 126.7 (d), 126.8 (d), 126.9 (d), 127.4 (d), 127.9 (d), 128.2 (d), 128.6 (d), 129.1 (d), 136.0 (s), 137.4 (s), 143.0 (s), 178.3 (s). IR (neat): ν = 3667, 3432, 2976, 2903, 1748, 1668, 1490, 1449, 1376, 1209, 1163, 1056, 1024 cm^{-1}. HRMS (ESI-Q-TOF): *m/z* Calcd for C$_{20}$H$_{19}$O$_3$ [M + H]$^+$: 307.1334; Found: 307.1333.

4-[hydroxy(phenyl)methyl]-4H-spiro[naphthalene-1,3′-oxolan]-2′-one (**20c**) **DS2**: Obtained as a white solid. Mp = 66–67 °C. R_f = 0.20 (PE/MTBE 2:1). ^{1}H NMR (500 MHz, CDCl$_3$): δ = 1.28 (bs, 1H), 2.64 (ddd, *J* = 13.7, 8.3, 5.0 Hz, 1H), 3.04 (ddd, *J* = 13.7, 9.0, 7.3 Hz, 1H), 3.97 (ddd, *J* = 4.6, 3.2, 1.4 Hz, 1H), 4.66 (ddd, *J* = 9.5, 8.3, 7.3 Hz, 1H), 4.74 (ddd, *J* = 9.5, 9.0, 5.0 Hz, 1H), 5.24 (d, *J* = 3.2 Hz, 1H), 5.80 (dd, *J* = 10.0, 4.6 Hz, 1H), 5.95 (dd, *J* = 10.0, 1.4 Hz, 1H), 7.31–7.44 (m, 9H). ^{13}C NMR (125 MHz, CDCl$_3$): δ = 38.0 (t), 48.4 (d), 48.5 (s), 66.5 (t), 77.7 (d), 125.7 (d), 125.9 (d), 126.3 (d), 127.1 (d), 127.5 (d), 127.8 (d), 128.2 (d), 128.6 (d), 128.7 (d), 135.5 (s), 135.9 (s), 143.0 (s), 179.8 (s). IR (neat): ν = 3439, 3030, 2922, 1761, 1510, 1450, 1374, 1268, 1165, 1024, 961, 759 cm^{-1}. HRMS (ESI-Q-TOF): *m/z* Calcd for C$_{20}$H$_{19}$O$_3$ [M + H]$^+$: 307.1334; Found: 307.1333.

4-[hydroxy(phenyl)methyl]-4H-spiro[naphthalene-1,3′-oxolan]-2′-one (**20c**) **DS3**: Obtained as a colorless liquid R_f = 0.18 (PE/MTBE 2:1). ^{1}H NMR (500 MHz, CDCl$_3$): δ = 1.70 (bs, 1H), 1.59 (ddd, *J* = 13.2, 7.3, 5.7 Hz, 1H), 2.21 (dt, *J* = 13.2, 7.7 Hz, 1H), 4.04 (dd, *J* = 5.6, 4.8 Hz,

1H), 4.30 (ddd, *J* = 9.3, 7.7, 7.3 Hz, 1H), 4.32 (ddd, *J* = 9.3, 7.7, 5.7 Hz, 1H), 5.02 (d, *J* = 5.6 Hz, 1H), 5.88 (d, *J* = 10.1 Hz, 1H), 6.23 (dd, *J* = 10.1, 4.8 Hz, 1H), 7.00–7.03 (m, 1H), 7.20–7.24 (m, 3H), 7.30–7.36 (m, 3H). ^{13}C NMR (125 MHz, CDCl$_3$): δ = 39.8 (t), 47.5 (d), 48.6 (s), 65.2 (t), 79.1 (d), 126.7 (d), 126.9 (d), 127.2 (d), 127.4 (d), 127.5 (d), 127.6 (d), 127.7 (d), 128.0 (d), 129.4 (d), 134.7 (s), 136.3 (s), 140.9 (s), 178.7 (s). IR (neat): ν = 3450, 3061, 3029, 2922, 1760, 1677, 1489, 1449, 1372, 1161, 1024, 909, 761 cm^{-1}. HRMS (ESI-Q-TOF): *m/z* Calcd for C$_{20}$H$_{19}$O$_3$ [M + H]$^+$: 307.1334; Found: 307.1346.

4-[hydroxy(phenyl)methyl]-4H-spiro[naphthalene-1,3′-oxolan]-2′-one (**20c**) **DS4**: Obtained as a white solid. Mp = 64–65 °C. R_f = 0.15 (PE/MTBE 2:1). ^{1}H NMR (500 MHz, CDCl$_3$): δ = 1.60 (bs, 1H), 2.61 (ddd, *J* = 13.6, 8.3, 5.1 Hz, 1H), 3.02 (ddd, *J* = 13.6, 8.7, 7.3 Hz, 1H), 3.87 (dd, *J* = 5.8, 5.0 Hz, 1H), 4.63 (ddd, *J* = 9.5, 8.3, 7.3 Hz, 1H), 4.71 (ddd, *J* = 9.5, 8.7, 5.01Hz, 1H), 4.95 (d, *J* = 5.8 Hz, 1H), 5.88 (d, *J* = 9.8 Hz, 1H), 5.97 (dd, *J* = 9.8, 5.0 Hz, 1H), 6.93 (dm, *J* = 7.8 Hz, 1H), 7.19 (tm, *J* = 7.8 Hz, 1H), 7.30–7.44 (m, 7H). ^{13}C NMR (125 MHz, CDCl$_3$): δ = 38.3 (t), 48.5 (d), 48.6 (s), 66.2 (t), 77.6 (d), 125.6 (d), 126.8 (d), 127.1 (d), 127.4 (d), 127.6 (d), 128.2 (d), 128.5 (d), 130.4 (d), 130.4 (d), 134.3 (s), 136.1 (s), 142.7 (s), 178.8 (s). IR (neat): ν = 3666, 3434, 2971, 2920, 1759, 1599, 1445, 1374, 1259, 1160, 1025, 909, 759 cm^{-1}. HRMS (ESI-Q-TOF): *m/z* Calcd for C$_{20}$H$_{19}$O$_3$ [M + H]$^+$: 307.1334; Found: 307.1334.

3.3.3. Analytical Data of Products **27** from Reactions with Benzophenone (**19**)

trans-8-[hydroxy(diphenyl)methyl]-2-oxaspiro[4.5]deca-6,9-dien-1-one (*trans*-**27a**): Obtained as a white solid. Mp = 225–226 °C. R_f = 0.28 (PE/MTBE 2:1). ^{1}H NMR (600 MHz, CDCl$_3$): δ = 1.58 (bs, 1H), 2.28 (t, *J* = 7.0 Hz, 2H), 4.24 (tt, *J* = 3.0, 2.1 Hz, 1H), 4.40 (t, *J* = 7.0 Hz, 2H), 5.81 (dd, *J* = 10.3, 2.1 Hz, 2H), 5.88 (dd, *J* = 10.3, 3.0 Hz, 2H), 7.25 (tm, *J* = 7.4 Hz, 2H), 7.35 (ddm, *J* = 8.3, 7.4 Hz, 4H), 7.57 (dm, *J* = 8.3 Hz, 4H). ^{13}C NMR (150 MHz, CDCl$_3$): δ = 37.3 (t), 44.2 (d), 46.0 (s), 65.3 (t), 79.3 (s), 125.6 (d), 127.0 (d), 127.9 (d), 128.2 (d), 128.5 (d), 144.9 (s), 177.1 (s). IR (neat): ν = 3446, 3026, 2919, 1754, 1489, 1446, 1167, 1021, 913, 846, 753 cm^{-1}. HRMS (ESI-Q-TOF): *m/z* Calcd for C$_{22}$H$_{19}$O$_2$ [M − H$_2$O + H]$^+$: 315.1385; Found: 315.1374.

cis-8-[hydroxy(diphenyl)methyl]-2-oxaspiro[4.5]deca-6,9-dien-1-one (*cis*-**27a**): Obtained as a white solid. Mp = 189–190 °C. R_f = 0.16 (PE/MTBE 2:1). ^{1}H NMR (600 MHz, CDCl$_3$): δ = 1.59 (bs, 1H), 2.38 (t, *J* = 7.0 Hz, 2H), 4.27 (tt, *J* = 3.8, 1.3 Hz, 1H), 4.46 (t, *J* = 7.0 Hz, 2H), 5.75 (dd, *J* = 10.3, 1.3 Hz, 2H), 5.80 (dd, *J* = 10.3, 3.8 Hz, 2H), 7.21 (tm, *J* = 7.4 Hz, 2H), 7.34 (ddm, *J* = 8.3, 7.4 Hz, 4H), 7.67 (dm, *J* = 8.3 Hz, 4H). ^{13}C NMR (150 MHz, CDCl$_3$): δ = 36.6 (t), 45.0 (d), 46.5 (s), 65.8 (t), 77.8 (s), 125.7 (d), 126.6 (d), 128.1 (d), 128.3 (d), 128.5 (d), 145.9 (s), 178.7 (s). IR (neat): ν = 3446, 3027, 2919, 1753, 1489, 1446, 1167, 1020, 913, 846, 753 cm^{-1}. HRMS (ESI-Q-TOF): *m/z* Calcd for C$_{22}$H$_{19}$O$_2$ [M − H$_2$O + H]$^+$: 315.1385; Found: 315.1372.

trans-8-[hydroxy(diphenyl)methyl]-6,7-dimethyl-2-oxaspiro[4.5]deca-6,9-dien-1-one (*trans*-**27b**): Obtained as a white solid. Mp = 189–190 °C. R_f = 0.28 (PE/MTBE 2:1). ^{1}H NMR (500 MHz, CDCl$_3$): δ = 1.18 (s, 3H), 1.57 (s, 3H), 2.11 (ddd, *J* = 13.2, 7.4, 3.5 Hz, 1H), 2.30 (bs, 1H), 2.51 (dt, *J* = 13.2, 9.2 Hz, 1H), 4.12 (dd, *J* = 4.5, 0.8 Hz, 1H), 4.35 (td, *J* = 9.2, 7.4 Hz, 1H), 4.41 (td, *J* = 9.2, 3.5 Hz, 1H), 5.83 (dd, *J* = 10.0, 0.8 Hz, 1H), 5.96 (dd, *J* = 10.0, 4.5 Hz, 1H), 7.27–7.37 (m, 8H), 7.52 (dm, *J* = 8.5 Hz, 1H), 7.60 (dm, *J* = 8.5 Hz, 1H). ^{13}C NMR (125 MHz, CDCl$_3$): δ = 16.0 (q), 20.6 (q), 35.6 (t), 50.9 (s), 51.6 (d), 65.6 (t), 79.6 (s), 125.3 (d), 127.0 (s), 128.0 (d), 128.1 (d), 128.2 (d), 129.5 (s), 145.4 (s), 177.9 (s). IR (neat): ν = 3523, 2920, 1749, 1447,m1375, 1170, 1026, 949, 910 cm^{-1}. HRMS (ESI-Q-TOF): *m/z* Calcd for C$_{24}$H$_{23}$O$_2$ [M − H$_2$O + H]$^+$: 343.1698; Found: 343.1657.

cis-8-[hydroxy(diphenyl)methyl]-6,7-dimethyl-2-oxaspiro[4.5]deca-6,9-dien-1-one (*cis*-**27b**): Obtained as a white solid. Mp = 176–177 °C. R_f = 0.26 (PE/MTBE 2:1). ^{1}H NMR (500 MHz, CDCl$_3$): δ = 1.10 (d, *J* = 0.5 Hz, 3H), 1.61 (bs, 1H), 1.68 (d, *J* = 1.0 Hz, 3H), 2.16 (ddd, *J* = 13.4, 7.7, 4.2 Hz, 1H), 2.77 (ddd, *J* = 13.4, 9.1, 8.4 Hz, 1H), 4.25 (dquint.q, *J* = 4.6, 1.0, 0.5 Hz, 1H), 4.44 (ddd, *J* = 9.3, 8.4, 7.7 Hz, 1H), 4.50 (ddd, *J* = 9.3, 9.1, 4.2 Hz, 1H), 5465 (dd, *J* = 9.9, 1.0 Hz, 1H), 5.80 (dd, *J* = 9.9, 4.6 Hz, 1H), 7.16–7.20 (m, 2H), 7.27–7.35 (m, 4H), 7.68–7.75 (m, 4H). ^{13}C NMR (125 MHz, CDCl$_3$): δ = 16.4 (q), 20.5 (q), 33.8 (t), 50.8 (s), 51.5 (d), 66.3

(t), 77.9 (s), 125.2 (d), 127.2 (s), 128.1 (d), 128.2 (d), 128.4 (d), 131.1 (s), 147.2 (s), 180.1 (s). IR (neat): ν = 3524, 2973, 2912, 1748, 1491, 1446, 1375, 1170, 1028, 948, 819, 746 cm^{-1}. HRMS (ESI-Q-TOF): m/z Calcd for $C_{24}H_{23}O_2$ [M − H_2O + H]$^+$: 343.1698; Found: 343.1702.

trans-4-[hydroxy(diphenyl)methyl]-4H-spiro[naphthalene-1,3′-oxolan]-2′-one (*trans-**27c***): Obtained as a white solid. Mp = 213–214 °C. R_f = 0.24 (PE/MTBE 2:1). ^{1}H NMR (500 MHz, CDCl$_3$): δ = 2.23 (bs, 1H), 2.47 (ddd, J = 13.1, 8.0, 6.4 Hz, 1H), 2.63 (ddd, J = 13.1, 7.9, 6.3 Hz, 1H), 4.51 (ddd, J = 9.4, 8.0, 6.3 Hz, 1H), 4.55 (ddd, J = 9.4, 7.9, 6.4 Hz, 1H), 4.74 (dd, J = 4.9, 0.8 Hz, 1H), 6.03 (dd, J = 10.1, 0.8 Hz, 1H), 6.26 (dd, J = 10.1, 4.9 Hz, 1H), 6.38 (dd, J = 7.9, 1.4 Hz, 1H), 6.86 (ddd, J = 8.3, 7.9, 1.4 Hz, 1H), 7.07 (dd, J = 7.9, 1.4 Hz, 1H), 7.19–7.42 (m, 9H), 7.64 (dm, J = 8.5 Hz, 2H). ^{13}C NMR (125 MHz, CDCl$_3$): δ = 40.0 (t), 49.0 (d), 49.2 (s), 65.6 (t), 81.0 (s), 126.0 (d), 126.1 (d), 126.6 (d), 126.7 (d), 127.0 (d), 127.3 (d), 127.4 (d), 127.9 (d), 128.4 (d), 129.2 (d), 129.8 (d), 130.8 (d), 133.5 (s), 137.4 (s), 144.5 (s), 145.3 (s), 179.0 (s). IR (neat): ν = 3520, 2975, 2913, 1751, 1490, 1446, 1373, 1163, 1024, 950, 828, 766, 744 cm^{-1}. HRMS (ESI-Q-TOF): m/z Calcd for $C_{26}H_{21}O_2$ [M − H_2O + H]$^+$: 365.1542; Found: 365.1533.

cis-4-[hydroxy(diphenyl)methyl]-4H-spiro[naphthalene-1,3′-oxolan]-2′-one (*cis-**27c***): Obtained as a white solid. Mp = 225–226 °C. R_f = 0.20 (PE/MTBE 2:1). ^{1}H NMR (500 MHz, CDCl$_3$): δ = 2.63 (ddd, J = 13.8, 8.8, 5.8 Hz, 1H), 2.94 (ddd, J = 13.8, 8.8, 6.5 Hz, 1H), 4.64 (ddd, J = 9.3, 8.8, 6.5 Hz, 1H), 4.73 (ddd, J = 9.3, 8.8, 5.8 Hz, 1H), 4.81 (bs, 1H), 4.88 (d, J = 4.9 Hz, 1H), 5.82 (d, J = 10.1 Hz, 1H), 6.18 (dd, J = 10.1, 4.9 Hz, 1H), 6.20 (d, J = 7.8 Hz, 1H), 6.83 (t, J = 7.8 Hz, 1H), 7.18–7.30 (m, 6H), 7.40 (t, J = 7.8 Hz, 2H), 7.54 (d, J = 7.8 Hz, 2H), 7.82 (d, J = 7.8 Hz, 2H). ^{13}C NMR (125 MHz, CDCl$_3$): δ = 40.6 (t), 50.0 (d), 50.2 (s), 68.2 (t), 80.8 (s), 126.08 (d), 127.5 (d), 127.6 (d), 127.9 (d), 128.1 (d), 128.3 (d), 128.8 (d), 129.2 (d), 129.7(d), 130.2 (d), 130.4 (d), 131.1 (d), 134.3 (s), 138.3 (s), 147.4 (s), 148.1 (s), 181.4 (s). IR (neat): ν = 3665, 2980, 2905, 1763, 1488, 1448, 1375, 1160, 1028, 758 cm^{-1}. HRMS (ESI-Q-TOF): m/z Calcd for $C_{26}H_{21}O_2$ [M − H_2O + H]$^+$: 365.1542; Found: 365.1560.

4. Conclusions

In conclusion, the photochemistry of β-γ-unsaturated spirolactones is remarkably different from other 1,4-cyclohexadienes. The interaction of the carbonyl group with the double bonds through space results in an absorption band at 230 nm. That allows direct excitations with UV-C light without any additives. We obtained only products of an oxa-di-π-methane rearrangement and no di-π-methane rearrangement or [2 + 2] cycloaddition was observed. This can be explained by a single pathway, confirmed by calculations. Although the yields are only moderate, because polymerization can compete, we isolated products in their analytically pure form and confirmed their structures using NOESY measurements and an X-ray structure. To the best of our knowledge, these are the first examples of oxa-di-π-methane rearrangements of lactones.

Photochemistry, in the presence of benzaldehyde, can be performed by irradiation with UV-B light. The intermediate radicals abstract hydrogen atoms from the allylic position, affording alcohols as coupling products. The Paternó–Büchi reaction was observed with dimethyl lactone **11b** as well, due to the electron-rich double bond. We were able to separate all isomers and products were isolated in their pure form.

Photochemistry, in the presence of benzophenone, gave the highest selectivities because only two diastereomers are formed. Furthermore, steric hindrance suppresses the Paternó–Büchi reaction. All products were isolated by simple crystallization or column chromatography in moderate yields and the relative configurations were assigned using NOESY measurements. Furthermore, we obtained three X-ray structures, confirming the stereochemistry unequivocally. Overall, the photochemistry of β-γ-unsaturated spirolactones is interesting from the mechanistic point of view and makes functionalized products accessible from benzoic acids in only a few steps.

Supplementary Materials: The following supporting information can be downloaded at: https://www.mdpi.com/article/10.3390/photochem3040025/s1 [30–39], Figure S1: Excited state of spirolactone **11a**; Figure S2: Geometries and energies of **BR4**, **BR2a**, **BR2b**, **BR3a**, **BR3b**; Figure S3: Geometries and energies of **P1**, **P2**; Figure S4: Photochemical Setup; S10–S36: NMR Spectra; S37–S51: X-ray Structure Analyses.

Author Contributions: Conceptualization, T.L.; methodology, T.L.; investigation, W.F.; reactions and purifications, W.F. and M.M.; synthesis of starting materials, T.K.-B.; X-ray structure determination, A.K. and E.S.; Calculations, P.W.; writing—original draft preparation, T.L.; writing—review and editing, T.L., P.W. and W.F. All authors have read and agreed to the published version of the manuscript.

Funding: This research received no external funding.

Data Availability Statement: The datasets generated during and/or analysed during the current study are available from the corresponding author on reasonable request.

Conflicts of Interest: The authors declare no conflict of interest.

References

1. Srinivasan, R.; White, L.S.; Rossi, A.R.; Epling, G.A. Organic photochemistry with 6.7-eV photons: 1,4-cyclohexadiene and 1,4-cyclohexadiene-3,3,6,6-d4. *J. Am. Chem. Soc.* **1981**, *103*, 7299–7304. [CrossRef]
2. Kumar, A.; Chowdhury, P.K.; Rama Rao, K.V.S.; Mittal, J.P. Real-time observation of concerted benzene formation in the infrared multiphoton dissociation of 1,4-cyclohexadiene. *Chem. Phys. Lett.* **1991**, *182*, 165–170. [CrossRef]
3. Kumar, A.; Naik, P.D.; Saini, R.D.; Mittal, J.P. Direct evidence of a radical channel in photodissociation of 1,4-cyclohexadiene with ArF laser at 193 nm. *Chem. Phys. Lett.* **1999**, *309*, 191–197. [CrossRef]
4. Zilberg, S.; Haas, Y. The photochemistry of 1,4-cyclohexadiene in solution and in the gas phase: Conical intersections and the origin of the "helicopter-type" motion of H2 photo-generated in the isolated molecule. *Phys. Chem. Chem. Phys.* **2002**, *4*, 34–42. [CrossRef]
5. Hixson, S.S.; Mariano, P.S.; Zimmerman, H.E. Di-π-methane and oxa-di-π-methane rearrangements. *Chem. Rev.* **1973**, *73*, 531–551. [CrossRef]
6. Zimmerman, H.E.; Armesto, D. Synthetic Aspects of the Di-π-methane Rearrangement. *Chem. Rev.* **1996**, *96*, 3065–3112. [CrossRef] [PubMed]
7. Zimmerman, H.E. Di-π-Methane Rearrangement. In *CRC Handbook of Organic Photochemistry and Photobiology*, 3rd ed.; Two Volume Set; CRC Press: Boca Raton, FL, USA, 2019; pp. 511–526, ISBN 9780429100253.
8. Tröster, A.; Bach, T. Triplet-sensitised di-π-methane rearrangement of N-substituted 2-azabarrelenones. *Chem. Commun.* **2019**, *55*, 302–305. [CrossRef]
9. Poplata, S.; Tröster, A.; Zou, Y.-Q.; Bach, T. Recent Advances in the Synthesis of Cyclobutanes by Olefin [2+2] Photocycloaddition Reactions. *Chem. Rev.* **2016**, *116*, 9748–9815. [CrossRef]
10. Jennings, W.; Hill, B. Photodimerization of norbornadiene using chromium hexacarbonyl. *J. Am. Chem. Soc.* **1970**, *92*, 3199–3200. [CrossRef]
11. Huang, D.-J.; Cheng, C.-H. [2 + 2] Dimerization of norbornadiene and its derivatives in the presence of nickel complexes and zinc metal. *J. Organomet. Chem.* **1995**, *490*, C1–C7. [CrossRef]
12. Malik, C.K.; Vaultier, M.; Ghosh, S. Copper(I)-catalyzed [2 + 2] photocycloaddition of nonconjugated alkenes in room-temperature ionic liquids. *Synthesis* **2007**, 1247–1250. [CrossRef]
13. Linker, T.; Fröhlich, L. Regio- and Diastereoselective Photooxygenation of Chiral 2,5-Cyclohexadiene-l-carboxylic Acids. *Angew. Chem. Int. Ed. Engl.* **1994**, *33*, 1971–1972. [CrossRef]
14. Vorndran, K.; Linker, T. Simple two-step ipso substitution of aromatic carboxylic acids by alkyl halides. *Angew. Chem. Int. Ed. Engl.* **2003**, *42*, 2489–2491. [CrossRef] [PubMed]
15. Krüger, T.; Vorndran, K.; Linker, T. Regioselective arene functionalization: Simple substitution of carboxylate by alkyl groups. *Chem.-A Eur. J.* **2009**, *15*, 12082–12091. [CrossRef]
16. Krüger, T.; Linker, T. Synthesis of γ-Spirolactams by Birch Reduction of Arenes. *Eur. J. Org. Chem.* **2021**, 1585–1591. [CrossRef]
17. Krüger, T.; Bramborg, A.; Kelling, A.; Sperlich, E.; Linker, T. Birch Reduction of Arenes as an Easy Entry to γ-Spirolactones. *Eur. J. Org. Chem.* **2021**, 6383–6391. [CrossRef]
18. Martin, H.-D.; Mayer, B. Proximity Effects in Organic Chemistry—The Photoelectron Spectroscopic Investigation of Non-Bonding and Transannular Interactions. *Angew. Chem. Int. Ed. Engl.* **1983**, *22*, 283–314. [CrossRef]
19. Czarnecki, M.; Wessig, P. Scaling Up UV-Mediated Intramolecular Photodehydro-Diels–Alder Reactions Using a Homemade High-Performance Annular Continuous-Flow Reactor. *Org. Process Res. Dev.* **2018**, *22*, 1823–1827. [CrossRef]
20. Zimmerman, H.E. Oxa-Di-π-Methane Rearrangement. In *CRC Handbook of Organic Photochemistry and Photobiology*, 3rd ed.; Two Volume Set; CRC Press: Boca Raton, FL, USA, 2019; pp. 527–548, ISBN 9780429100253.

21. Swenton, J.S.; Madigani, D.M. Competitive hydrogen and carbomethoxy migration in the photochemistry of 7-carbomethoxy-3,4-benzotropilidene. *Tetrahedron* **1972**, *28*, 2703–2716. [CrossRef]
22. Becker, H.G.O. *Einführung in Die Photochemie*; Deutscher Verlag der Wissenschaften: Berlin, Germany, 1991; ISBN 3136337026.
23. Fréneau, M.; Hoffmann, N. The Paternò-Büchi reaction—Mechanisms and application to organic synthesis. *J. Photochem. Photobiol. C Photochem. Rev.* **2017**, *33*, 83–108. [CrossRef]
24. D'Auria, M. Paternó-Büchi Reaction. In *CRC Handbook of Organic Photochemistry and Photobiology*, 3rd ed.; Two Volume Set; CRC Press: Boca Raton, FL, USA, 2019; pp. 653–681.
25. D'Auria, M. The Paternò-Büchi reaction—A comprehensive review. *Photochem. Photobiol. Sci.* **2019**, *18*, 2297–2362. [CrossRef] [PubMed]
26. Bradshaw, J.S. Ultraviolet Irradiation of Carbonyl Compounds in Cyclohexene and 1-Hexene. *J. Org. Chem.* **1966**, *31*, 237–240. [CrossRef]
27. Griesbeck, A.G.; Stadtmüller, S. Photocycloaddition of Benzaldehyde to Cyclic Olefins: Electronic Control of Endo Stereoselectivity. *J. Am. Chem. Soc.* **1990**, *112*, 1281–1283. [CrossRef]
28. Andreu, I.; Neshchadin, D.; Rico, E.; Griesser, M.; Samadi, A.; Morera, I.M.; Gescheidt, G.; Miranda, M.A. Probing lipid peroxidation by using linoleic acid and benzophenone. *Chem.—Eur. J.* **2011**, *17*, 10089–10096. [CrossRef]
29. Zipse, H. Radical Stability—A Theoretical Perspective. In *Radicals in Synthesis I*; Gansäuer, A., Ed.; Springer: Berlin/Heidelberg, Germany, 2006; pp. 163–189, ISBN 978-3-540-31330-4.
30. Yu, H.S.; He, X.; Li, S.L.; Truhlar, D.G. MN15: A Kohn-Sham Global-Hybrid Exchange-Correlation Density Functional with Broad Accuracy for Multi-Reference and Single-Reference Systems and Noncovalent Interactions. *Chem. Sci.* **2016**, *7*, 5032–5051. [CrossRef] [PubMed]
31. Rassolov, V.A.; Ratner, M.A.; Pople, J.A.; Redfern, P.C.; Curtiss, L.A. 6-31G* Basis Set for Third-Row Atoms. *J. Comp. Chem.* **2001**, *22*, 976–984. [CrossRef]
32. Frisch, M.J.; Trucks, G.W.; Schlegel, H.B.; Scuseria, G.E.; Robb, M.A.; Cheeseman, J.R.; Scalmani, G.; Barone, V.; Mennucci, B.; Petersson, G.A.; et al. *Gaussian 16, Revision C.01*; Gaussian, Inc.: Wallingford, CT, USA, 2019.
33. Adamo, C.; Jacquemin, D. The calculations of excited-state properties with Time-Dependent Density Functional Theory. *Chem. Soc. Rev.* **2013**, *42*, 845. [CrossRef]
34. Laurent, A.D.; Adamo, C.; Jacquemin, D. Dye chemistry with time-dependent density functional theory. *Phys. Chem. Chem. Phys.* **2014**, *16*, 14334–14356. [CrossRef]
35. STOE & Cie GmbH, X-Area. *Software Package for Collecting Single-Crystal Data on STOE Area-Detector Diffractometers, for Image Processing, for the Correction and Scaling of Reflection Intensities and for Outlier Rejection*; STOE & Cie GmbH: Darmstadt, Germany, 2018.
36. Sheldrick, G.M. A Short History of SHELX. *Acta Cryst. Sect. A Found. Crystallogr.* **2008**, *64*, 112–122. [CrossRef]
37. Sheldrick, G.M. Crystal Structure Refinement with SHELXL. *Acta Cryst. C* **2015**, *71*, 3. [CrossRef]
38. Kratzert, D. FinalCif. Available online: https://dkratzert.de/finalcif.html (accessed on 23 September 2023).
39. Brandenburg, K.; Putz, H. *Diamond. Crystal and Molecular Structure Visualization*; Crystal Impact: Bonn, Germany, 2020.